Modelling the impact of polymer swelling on production, reactor behaviour and polymer particle size distribution of polyethylene

Alves, Rita[1]

[1]Instituto Superior Técnico, Universidade Técnica de Lisboa, 1049-0901 Lisboa, Portugal

Abstract

The present work studies the impact of polyethylene swelling in reactor behaviour and polymer particle size distribution. This study is carried out by adding an inert alkane to polyethylene production in gas-phase and dry mode.

The developed model estimates de polyethylene production and reactor's conditions, such as temperature and bed porosity in steady-state. Ethylene concentration in the active sites is estimated using the Sanchez-Lacombe EOS thermodynamic model

The model was validated through comparison with patent US 6864332 B2. By the results, it is possible to conclude that the presence of an inert alkane increases reactor production, decreases reactor temperature and increases mean particle size. The bigger the alkane molecule size, the more noticeable the effects are.

Keywords: Polyethylene, Gas-phase, Dry mode, FBR modelling, Particle Size distribution, swelling.

Introduction

Polyethylene (PE) is a polyolefin consisting, in its simplest form, of a long backbone chain with an even number of carbon atoms (covalently linked) and two hydrogen atoms attached to each carbon, ending in methyl groups. Polyethylene resins can be organized into three main categories: high density polyethylene (HDPE), low density polyethylene (LDPE) and linear low density polyethylene (LLDPE) [1].

Industrial processes for the production of polyethylene (PE) can be divided into different categories according to the phase in which the polymerization takes place: solution, slurry, gas-phase processes, with the latter two being more significant in terms of production volumes. While slurry phase processes are commercially important for a number of reasons, gas-phase processes are even more widely used due to their versatility. They can be used to produce resins with a full range of densities, from LLDPE to HDPE in the same process [2]. The only type of reactor used for the production of different grades of PE in the gas phase are fluidized bed reactors (FBR) since this is the only type of reactor that allows one to achieve commercially pertinent rates of polymerization and at the same time to allow sufficient evacuation of energy from the reactor [1].

A diagram of a typical FBR for PE production is shown in Figure 1. The reactor is essentially an empty cylinder with an expansion zone at the top (to reduce the gas velocity and help remove any fine particles from flowing out of the reactor and into the recycle compressor), and a distributor plate at the bottom. Catalyst (or prepolymerized catalyst) is fed into the reactor slightly above the distributor plate, and the fluids are typically fed through the bottom of the reactor, usually (but not always) below the distributor plate. The polymer is removed through a product discharge valve, following into a series of degassing tanks to separate the unreacted monomer and afterwards into a purge column to remove and recycle any residual monomer, and deactivate the catalyst. The recovered unreacted monomer, along with the gaseous outlet of the reactor is compressed, cooled and afterwards mixed with fresh monomer, hydrogen and eventually other compounds, then recycled to the reactor.

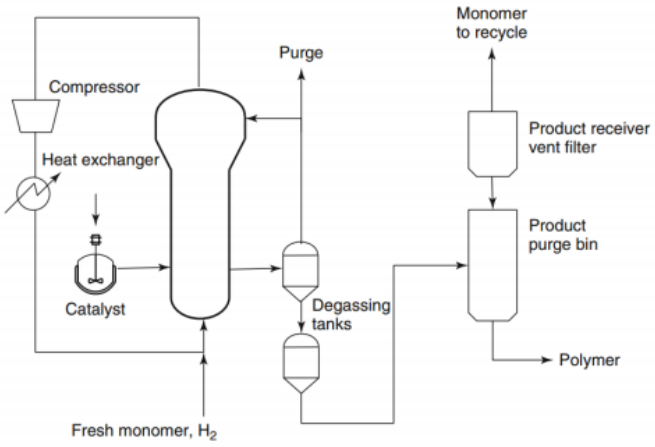

Figure 1. Unipol process for polyethylene production. Adapted from [2]

One of the key points in the safe and economical operation of an FBR for the production of PE is heat removal; a typical commercial scale reactor will generate several 10s of megawatts of energy during polymer production, and since PE can melt if there are temperature excursions, overheating can pose a serious problem to smooth operation, and eventually limit the rate of polymerization. It is well-known that most of the heat generated by the polymerization is removed via the gas phase as it flows over the particles in the bed. However, this way of cooling the bed is limited by the maximum flow rate of gas through the bed; if the flow is too low, the bed collapses, and if it is too high, a significant fraction of the particles will be blown out of the bed and into the recycle stream. The only other means of improving the heat removal capacity of the reactor is to alter the physical nature of the feed stream. One particular way of doing this is to include chemically inert

alkane components in the feed stream to the reactor, with higher heat capacity than ethylene and nitrogen (the main components of the gas phase in such reactors). When the reactor is operated in “dry mode”, adding compounds such as ethane, propane or butane in vapour form can be used for this purpose (higher alkanes can be used as well, but then the feed stream can only be cooled so far without condensation taking place). Such compounds are often referred to as induced condensing agents (ICA).

Although the initial purpose of adding ICA to the reactor is to regulate the liquid stream dew point and/or increase vapour stream heat capacity, there is another noticeable consequence of great interest as well: the ICA is considerably absorbed by the polymer phase. This absorption is observed to be primarily a function of the fraction of ICA in the gas phase, but also a function of the amorphous phase polymer density. This phenomena has two main consequences: it alters the polymer physically and it changes the ethylene/polymer equilibrium [3][4].

The adsorption of ICA into the polyethylene is observed to modify the polymer physically, by swelling and plasticizing it, as well as increasing its density. There are temperature gradients within the individual particles when they are actively producing polymer. The equilibrium absorption of the ICA into the polymer decreases with the increase of temperature. The desorption involves a latent heat similar to evaporation. Thus, when particles reach a hot region and begin to overheat, some ICA will desorb from the polymer, causing a cooling effect [3]. The ICA can also effect mass transfer, as its presence widens the polymer particles, aiding the transport of components in and out of the particles. This is of the upmost importance, since the vast majority of the active sites are not in the outer surface of the catalyst/polymer particle. The delivery and withdrawal of species having a relatively high thermal conductivity may become a mechanism of cooling the micro-particle clusters [4].

The polymer/ICA/ethylene system has an interesting interaction between the different components, especially when analysing the effect that the ICA has on the ethylene solubility in the polymer. To study this system interactions, a thermodynamic model is required to properly describe these interactions. In the present work the Sanchez-Lacombe Equation of State as the polymer-penetrant thermodynamics are non-ideal [2][5].

Since fluidized beds are widely used in many forms, one can find numerous models for predicting their behaviours in the open literature [6][7][8]. Such studies describe fluidized beds in great detail and provide an extensive list of empirical correlations which may be used to estimate properties of importance when designing fluidized bed reactors. Studies on the modelling of FBRs in the specific case of PE production are extremely numerous as well, and exhibit many levels of complexity [9] [10] [11] . Since this works focus only on investigating the impact of adding an ICA on the overall reactor behaviour, we will use a simplified approach and treat the FBR as a continuous stirred tank reactor. It has been shown elsewhere that this simplification has a limited impact on the calculation of the final PSD and conversion in the reactor [12].

The supported catalysts used in the polyolefin industry are highly porous particles with typical diameters in the order of 10–100 μm [2]. The supported catalyst particle (macrograin or macroparticle) is composed of an assembly of smaller structures, often referred to as micrograins (also called microparticles) [2][13][14]. While interest in other support types is growing, $MgCl_2$ and SiO_2 are essentially the only commercially used supports at the present time.

The particle growth begins with a process referred to as particle fragmentation. As shown in Figure 2, when the reactive species reach the active sites, they start to react, forming polymer layers inside the pores of the catalyst particle, and the structure of the particle begins to evolve. As polymer accumulates at the active sites, the inorganic phase suffers a local build-up of stress at different points, and very quickly fragments into a series of unconnected mineral substructures held together by a polymer phase. This process continues throughout the entire support as monomer keeps reaching the active sites and polymer builds up. This kind of fractioning is well known and described in several references [14][15][16][17].

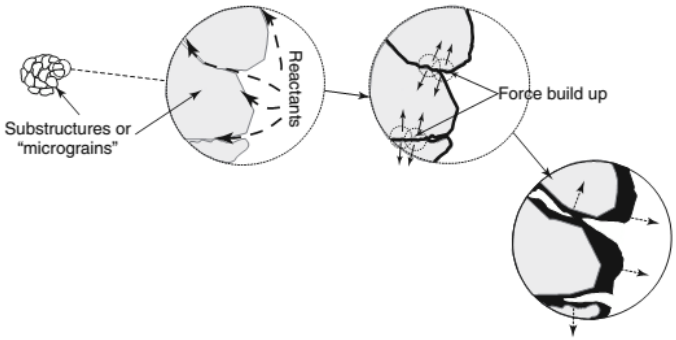

Figure 2. Particle growth evolution. Adapted from [2].

One consequence of this catalyst fragmentation mechanism is the replication phenomenon, where the PSD shape of the polymer particles is duplicated by the polymer PSD. This is a very important phenomenon, since it allows to easily predict the polymer PSD [2][18][19]..

Once fragmentation occurs, the particle growth step begins. The polymer particle grows by expansion: the newly formed polymer at the active sites displaces the previously formed polymer [2].

There are several models in the open literature that describe the particle growth and polymer particle size distribution [10][20][21].

Model Description

The present model consists of the merging and upgrading of two existing models developed by Cecílio

[22]. The base models consist of a Particle Size Distribution (PSD) model and a gas-phase polyethylene FBR model. The PSD model calculates the PSD of the polymer particles produced with heterogeneous Ziegler-Natta catalysts. The model developed by Cecílio [22] is adapted for a slurry phase reactor. However, a simple adaptation can be made to apply the same model in FBR's. The reactor model emulates the behaviour of a FBR reactor for the production of polyethylene.

The model presented in the following section describes the operation of a gas-phase HDPE production reactor in dry mode through a series of mass and heat balances.

Reactor Model

The mass and heat balances in the present model are based on a set of problem definitions and assumptions, described below.

Problem Definition:

- 1 gaseous inlet consisting of ethylene, an inert heavy alkane and nitrogen;
- 1 solid inlet stream consisting of catalyst particles, with negligible amounts of carrier;
- 1 gaseous outlet containing non-reacted ethylene, inert heavy alkane and nitrogen;
- 1 solid outlet containing the polymer phase, consisting of the polymer and catalyst particles with dissolved ethylene and alkane;
- Due to the heat transfer, 2 different outlet temperatures are considered, one for the gaseous outlet (T_b)and another for the polymer phase outlet (T_s);

Assumptions:

- The residence time distribution of the particles is assumed to be that of an CSTR operating in steady-state;
- The catalyst particles are considered spherical;
- Catalyst activation is considered to be instantaneous;
- Elutriation of solids is neglected;
- The thermodynamic equilibrium is achieved instantaneously and the polymer particles are considered fully mature;
- The gas-phase keeps a constant concentration of ethylene, nitrogen and ICA;
- Ethylene and ICA solubility dependence on temperature is neglected within each range of temperature;
- Nitrogen solubility in the polymer phase and impact on ethylene solubility are neglected;
- Convective heat transfer is considered between the catalyst/polymer particles and the bulk gaseous phase;

All gas thermal properties were obtained using correlations from Reid et al. [9].

The reaction rate assumed for the polymerization was proposed by Floyd and is written as follows:

$$R_p = k_p \cdot C^* \cdot C_{Et}^P \quad (1)$$

$$C^* = \frac{C_0^*}{1 + k_d \cdot \frac{V_C}{Q_c}} \quad (2)$$

Where $k_p$represents the kinetic rate constant, C^* is the active sites concentration on the catalyst (given by equation (2)) and C_{Et}^P represents the ethylene concentration inside the polymer phase. This last parameter is of the utmost importance and an estimation is needed in order to predict the polymer production. In equation (2), C_0^* is the initial active sites concentration and $\frac{V_C}{Q_c}$ can be interpreted as the catalysts residence time.

The resulting mass balances are applied to the various compounds, namely: ethylene and ICA, accounting for the amount solubilized in the polymer; nitrogen and the polyethylene; and the catalyst's active sites concentration. It is important to mention the use of Arrhenius Law to predict catalyst deactivation and the kinetic rate constant at the reaction temperature.

The production of PE is estimated according to the following expression (kg/s):

$$Q_{PE} = R_p \cdot V_c \cdot MW_{et} \quad (3)$$

The catalyst productivity is defined by equation (4) ($g_{polymer}/g_{catlyst}$):

$$Productivity = \frac{Q_{PE}}{Q_C} \quad (4)$$

Inside the reactor two temperatures can be observed: The bulk temperature (T_b) and the solid particles temperature (T_s). Therefore, two heat balances are required, one to the solid particles and one to the reactor global heat.

The heat balance to the solid particles can be written as follows:

$$\Delta H_{polym} = h \cdot A_p \cdot (T_s - T_b) \quad (5)$$

Where ΔH_{polym} is the heat of reaction, h represents the convective heat transfer coefficient (estimated according to [23]) and A_p the heat transfer area.

The reactor general heat balance is written as follows:

$$\Delta H_{in} - \Delta H_{out} + \Delta H_{generated} = \Delta H_{accumulation} \quad (6)$$

Reference State:

- Reference Temperature – Inlet Temperature (T_{in});
- Reference Pressure – Reactor working pressure;
- Gaseous ethylene, nitrogen and alkane;
- Solid catalyst;
- Amorphous polyethylene.

Assuming this reference state and that the operation is occurs in steady state, the heat balance in equation (6) is reduced to:

$$-\Delta H_{out} + \Delta H_{generated} = 0 \quad (7)$$

The pressure drop was calculated using Ergun's equation [24].

The superficial velocity, u_{mf}, is the minimum superficial gas velocity at which fluidization occurs. The terminal velocity of the particles (u_t) is the velocity at which transport occurs and both were estimated using the methods presented in [8].

The porosity of the bed was predicted in a simplistic fashion by taking advantage of the linear relationship between the superficial velocity and the bed porosity.

With the u_{mf} and u_t a linear relationship between the bed porosity and the superficial velocity was found. The bed porosity is then calculated with this new found equation, using the superficial velocity (see Figure 3).

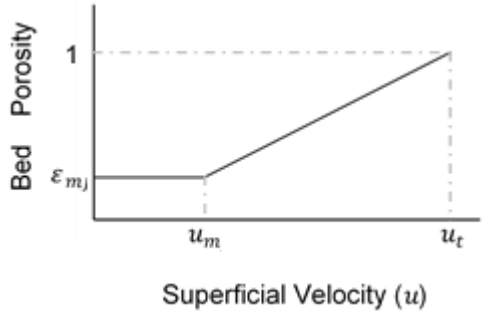

Figure 3. Bed porosity vs Fluid superficial velocity (adapted from [8][25])

The superficial velocity (u) (m/s) is obtained in the usual manner:

$$u = \frac{Q_v}{A_S} \tag{8}$$

Where Q_v represents the volumetric flow and A_S the reactor's cross area.

Particle Size Distribution

Soares model [18] was developed for CSTR. However, one of the main assumptions in this work is that the RTD of the solids for the considered FBR is approximated to the one of a CSTR. The model equations developed by Soares [18] remain applicable.

The following assumptions were made when developing this model [18]:

- All active sites on the catalyst have the same propagation constant;
- The concentration of active sites is uniform throughout the catalyst and polymer particles;
- The catalyst possesses only stable active sites that do not suffer deactivation;
- The catalyst particle shape is considered to be a sphere;

The particle size can be obtain using equation (10):

$$d_p = d_c\,(1 + \alpha\, t)^{1/3} \tag{9}$$

Correspondent to this particle size, there is a particle population given by equation (11).

$$F(d_p) = \frac{3(1 + \alpha\, t)^{1/3}}{\alpha\, D_c}\frac{e^{-t/\tau}}{\tau} \tag{10}$$

Wherein,

$$\alpha = \frac{k_p\, C_{Et}^P\, C^* MW_{Et}}{\rho_{pol}} \tag{11}$$

Where D_p is the diameter (cm) of the polymer particle, D_c is the diameter of the catalyst particle (cm), t is the reaction time (min), τ is the average residence time of the reactor (min) and α is a combined kinetic parameter. In equation (12) k_{prop} is the average propagation constant ($cm^3.mol^{-1}.min^{-1}$), C_{Et}^P is the monomer concentration in the polymer phase (at the active sites) ($mol.cm^{-3}$), C^* is the active sites concentration in the catalyst ($mol.cm^{-3}$), MW_{Et} is the molar mass of the monomer ($g.mol^{-1}$) and ρ_{pol} is the specific weight of the obtained polymer ($g.cm^{-3}$).

However, the main limitation of the model, is that it was developed for one catalyst particle, while in reality the catalyst presents its own PSD. As such, an algorithm was developed to discretize the PSD and include de importance of this contribution.

The algorithm starts with the establishment of small intervals to categorize the polymer particles. Then, for each catalyst size, the polymer particle size is compared to the intervals frontiers to decide if it fits in that interval. If it does, then the population in that interval increases, but not before it is affected with the volume fraction corresponding to its original inlet catalyst. This allows for a more comprehensive view of the particle size distribution of the polymer that is being produced, by simulating a catalyst feed with different particle sizes.

From the particle size distribution, it is also possible to obtain the most common particle size of the polymer phase, which is considered to be particle diameter (d_p) for all calculations. For this step, an algorithm was developed that compares the population of each interval and selects the one with the largest population.

Model Implementation

The model was implemented using Matlab®. For the development of the code, there were two main concerns: The need to use a solver that allows a set of non-linear equations and the need to iterate the mean particle size (d_p), since the mean diameter of the particles is obtained from the polymer PSD, which is computed after the reactor equations.

To solve the reactor equations, Matlab's Optimization Toolbox's fsolve function was used. This function requires a matrix with the initial guess for every variable, since all the equations are solved simultaneously. Consequently, an auxiliary and simplified version of the model was developed in Microsoft Excel® to obtain the required initial values.

To assemble the model an iterative cycle is proposed, as seen in Figure 4.

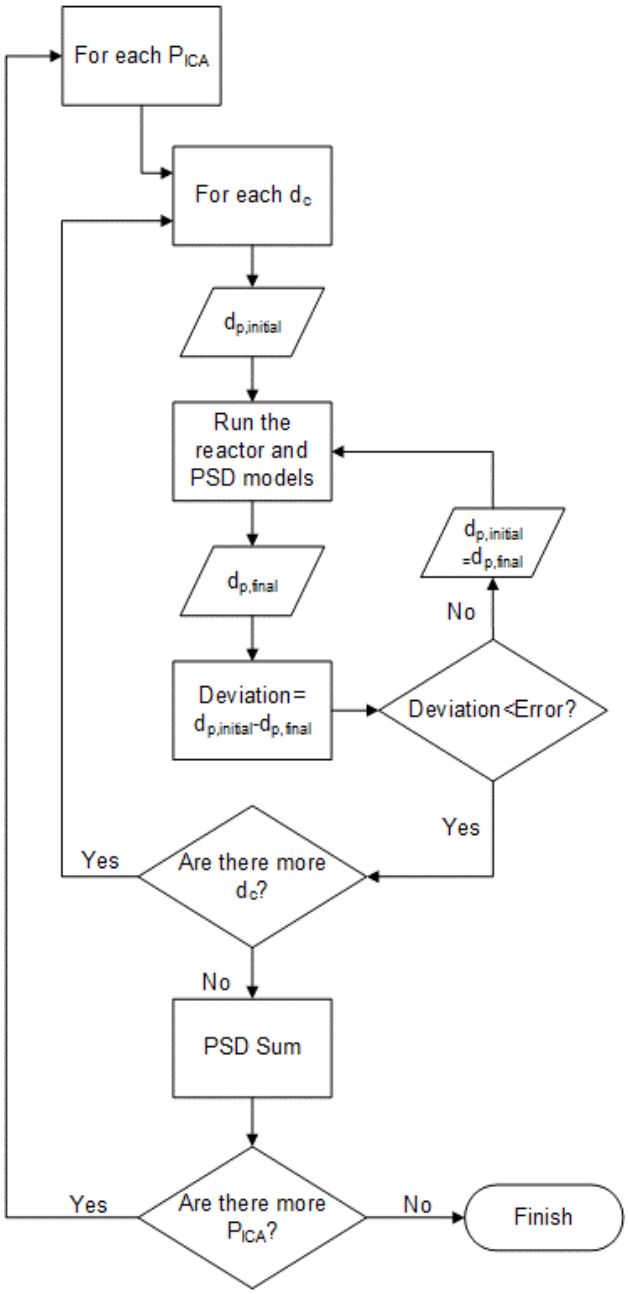

Figure 4. Main iterative cycle flowchart.

Results

The common parameters used in all simulations are summarized in Table 1. The properties of the gas phase calculations were based on[23][26].

ICA effect on ethylene solubility and polymer density

Using the SL-EoS based solubility and polymer phase density, concentration of each gaseous component in the polymer phase and amorphous polymer density in ternary systems was calculated and the results are shown in Figures 5 and 6. The increase in the ICA partial pressure in the gas phase leads to the increase of ethylene concentration in the polymer phase. In addition, the higher the carbon number of the ICA the higher is the ethylene concentration in the polymer phase at the same conditions. This observation can be attributed to the co-solvent effect of alkanes on the solubility of ethylene which manifest itself in multicomponent gases/polymer systems and is well known in the open literature. An increase in temperature leads to lower ethylene solubility in the polymer phase.

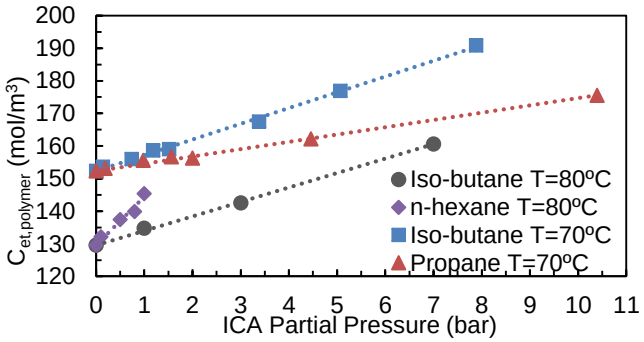

Figure 5. ICA effect on the concentration of ethylene in the polymer phase at 70º C and 80º C obtained from the SL-EoS in ternary (ethylene(1)/ICA(2)/PE(1)) systems.

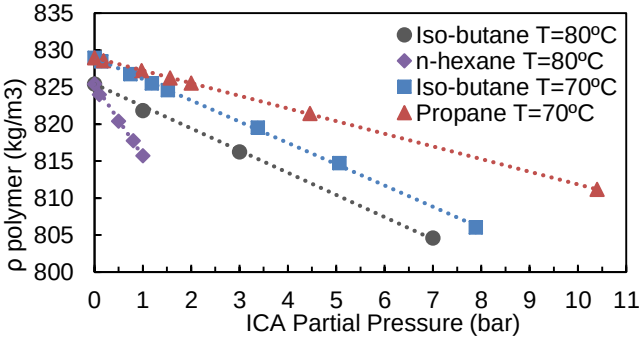

Figure 6. ICA effect on polymer density at 70ºC and 80ºC obtained from the SL-EoS in ternary (ethylene(1)/ICA(2)/PE(1)) systems.

From Figure 6 it can be noticed that the higher the carbon number of the ICA the lower is the polymer phase density at given conditions which is in agreement with the discussion made above. For the ease of calculations, correlations were developed for the ethylene and ICA concentration in the polymer phase (C_{Et}^{P} and C_{ICA}^{P}) and the polymer density.

Model Validation

The model validation was carried out by replicating the example 7C of the patent US 6,864,332 B2 [27]. The data used is shown in table 2.

Table 1. Data used in the validation of the model [27].

Reactor Abs. Pressure (bar)	22.4
Inlet Temperature (ºC)	35
Inlet gas flowrate (kg/s)	335
Inlet Catalyst flowrate (kg/s)	0.0024
Ethylene Partial Pressure (bar)	7.8
Propane Partial Pressure (bar)	4.3
Iso-butane Partial Pressure (bar)	3.3

Table 2. Properties of the solid phase, reaction parameters and reactor properties.

Parameter	Units	Value	Reference
Reactor Diameter, d	m	4.75	[27]
Reactor Bed Height, h_b	m	13.3	[27]
Catalyst type	-	Ziegler Natta	[28]
Catalyst Particle Diameter, d_c	µm	49; 55; 63	[28]
Initial Catalyst Active Site Concentration, C_0*	mol/m^3_c	0.52	[28]
Catalyst Density, ρ_c	kg/m^3	2300	[28]
Catalyst Heat Capacity, $Cp_{,c}$	J/(kg.K)	2000	[28]
Polymer Heat Capacity, $Cp_{,p}$	J/(kg.K)	2000	[28]
Kinetic rate constant, k_p ^{80ºC}	m^3/(mol.s)	180	[28]
Kinetic propagation constant, k_{prop}	m^3/(mol.min)	1.87x10^{10}	[28]
Catalyst deactivation rate constant, k_d ^{80ºC}	s^{-1}	1 x 10^{-4}	[28]
Reaction Activation Energy, E_a	J/mol	42000	[28]
Catalyst Deactivation Energy, E_d	J/mol	42000	[28]
Heat of Reaction, ΔH_{pol}	J/mol	-107600	[28]
Minimum Fluidized Bed Porosity, $\varepsilon_{m.f.}$	-	0.476	[8]
Reference Temperature T_{ref}	K	80	-

Since in the example there are two ICA, some minor alterations were made to the reactor equations. All equations regarding the ICA are still written in the same fashion, but accounting for two ICA compounds instead of one. For the ethylene concentration in the amorphous polymer (C_{Et}^P), a blunt approximation was made. C_{Et}^P is estimated using a combination of the equations obtained for each of the separate ICA. The solubility of ICA in the polymer was considered to not be affected by the presence of another ICA.

The following Table 3 shows the comparison between the results presented in example 7C [27] and the results obtained in the simulation.

Table 3. Comparison between the results presented in example 7C [28] and the simulation (Sim.) and the corresponding variation (Δ).

	7C	Sim.	Δ (%)
PE Production Rate (ton/h)	28.9	30.1	4.2
Reactor Temperature (ºC)	88	88	0.0
Superficial Velocity (m/s)	0.75	0.75	0.0

Analysing the results presented it is evident that the developed model is a good approximation of reality. The slight difference in the polyethylene production rate can be explained by use of a different catalyst and due to the solubility values only availability at 70ºC for propane and 80ºC for iso-butane and the reactor operates at 88ºC. Based on the current results and available information, the model can be considered reasonably valid.

Simulation I

The initial simulation considered a fixed inlet catalyst and gas flow and aim to disclose how the presence of ICA affects the reactor's parameters, such as temperature, rate of production, ethylene conversion and product PSD. Table 4 summarizes the used values. Nitrogen was used to achieve the desired reactor pressure and keep it constant throughout the simulations.

The results for simulation I are presented in Figures 7 to 11.

Table 4. Simulation I reactor parameters.

Reactor Abs. Pressure (bar)	20
Inlet Temperature (ºC)	35
Inlet gas flowrate (mol/s)	10000
Inlet Catalyst flowrate (kg/s)	0.0011
Ethylene Partial Pressure (bar)	7
Propane Partial Pressure (bar)	0 to 7
Iso-butane Partial Pressure (bar)	0 to 4

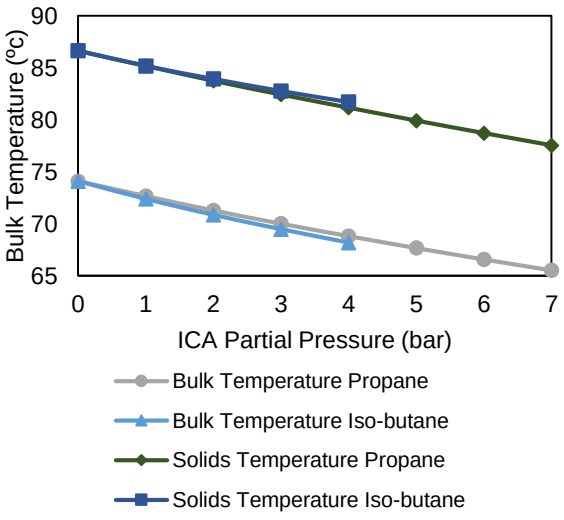

Figure 7. Effect of ICA on reactor bulk and solids temperature for simulation I.

In Figure 7 the temperature decreases with the increase of ICA. This is due to the ICA increasing the global specific heat of the gas-phase. It is possible to

observe that for the same pressures, iso-butane has a slightly higher cooling effect. This happens because specific heat of iso-butane is higher than the specific heat of propane. It is also interesting to observe that although the bulk temperature of the reactor when using iso-butane is lower than when using propane, the solids temperature is higher when compared to the propane simulation. This can be explained by the more pronounced co-solubility effect that iso-butane has in the system. The bigger the effect of co-solubility, the higher ethylene concentration in the polymer phase. That leads to higher PE production rates, which releases more heat of reaction. Figure 8 shows the effect of ICA in the PE production rate.

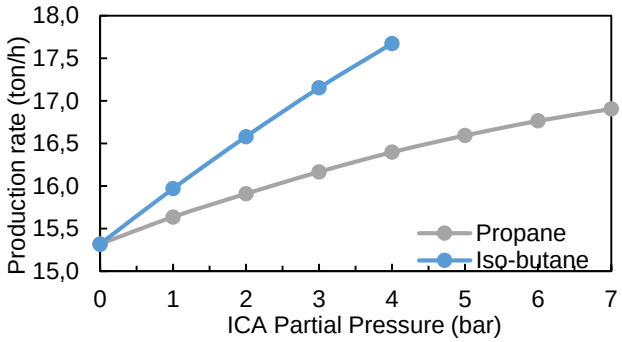

Figure 8. Effect of ICA on PE Production rate.

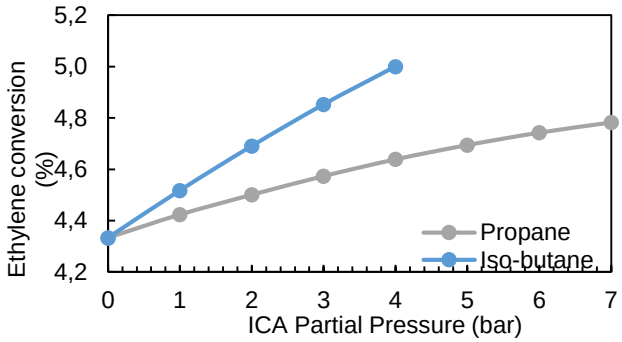

Figure 9. Effect of ICA on ethylene per pass conversion. Values regarding simulation I.

Figures 8 and 9 allows to conclude that the production rate, and consequently the ethylene conversation, increase with the presence of more ICA, which consolidates the results shown in Figure 7.

It is interesting to observe the different shapes of the curves. This is a result of the different effect that iso-butane and propane have on the ethylene solubility in the polymer phase. Iso-butane is a bigger molecule and induces a higher co-solubility effect than propane.

. In terms of production rate, using 4 bar of propane leads to a 7% increase. Contrasting with this value, the same amount of iso-butane leads to a 15% increase. In fact, even when using 7 bar of propane, the production is still lower than when using 4 bar of iso-butane. This is again a direct consequence of the co-solubility effect.

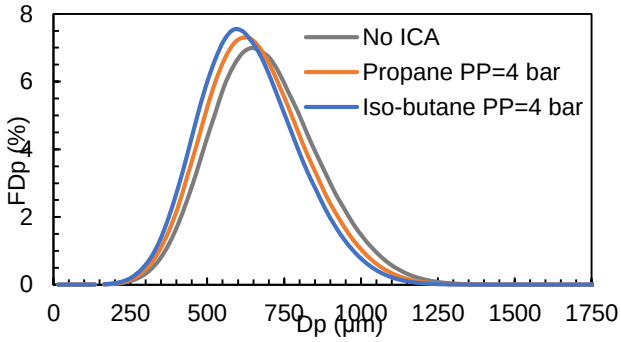

Figure 10. Effect of ICA on polymer PSD for simulation I.

In this simulation the mean particle size of the polymer decreases with the increase of ICA. This is a consequence of the solids temperature decrease, a highly important parameter in the PSD algorithm. In fact, an increase in the mean particle size could also be expected. Analysing the PSD equations (9) to (11), it is easy to assume that the increase in ICA partial pressure would lead to bigger particle sizes. However, the rise in ICA partial pressure and consequent increase in ethylene solubility in the polymer phase are proven to have a less significant effect than the solids temperature in the polymer PSD model. This can also be seen in Figure 19.

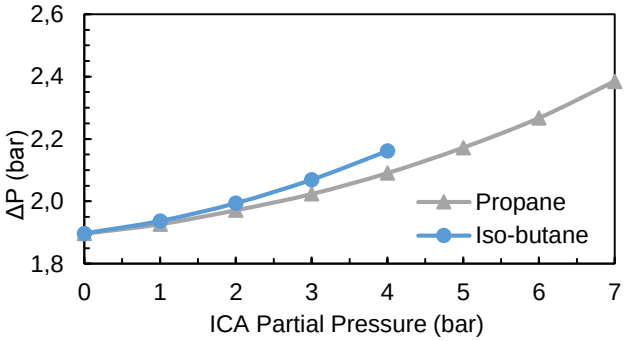

Figure 11. Effect of ICA on reactor pressure drop for simulation I.

The pressure drop in the reactor increases with the increase of ICA present. This is an expected behaviour. Ergun's equation [24] shows that the decrease of particle size will lead to the increase of pressure drop. As seen from Figure 10 the mean particle size decreases with the increase of ICA, leading to a higher pressure drop.

Both the superficial velocity and bed porosity maintained constant values regardless of the ICA pressure and alkane used. The simulation presents a bed porosity of 0.6 and a superficial velocity of 0.8 m/s.

Simulation II

Simulation II consist of keeping the reactor production rate and temperature constant while varying the partial pressure of ICA. This allows to understand better the implications of adding ICA into a current process, since the production rate might need to be kept in the existing facility. The values used in this simulation are presented in table below.

Table 5. Simulation III reactor parameters.

Reactor Abs. Pressure (bar)	20
Inlet Temperature (ºC)	35
Reactor temperature (ºC)	70
PE Production rate (ton/h)	15.8
Ethylene Partial Pressure (bar)	7
Propane Partial Pressure (bar)	0 to 9
Iso-butane Partial Pressure (bar)	0 to 4

The results for this simulation are presented in figures 12 to17.

The results obtained in Figure 12 and 13 are expected. Since the ICA has a cooling effect in the reactor (see Figure 7), it is necessary to decrease the inlet gas flowrate to maintain the temperature at 70ºC. However, a decrease in the inlet flowrate leads to a decrease in production. Therefore, it is also necessary to increase the catalyst feed.

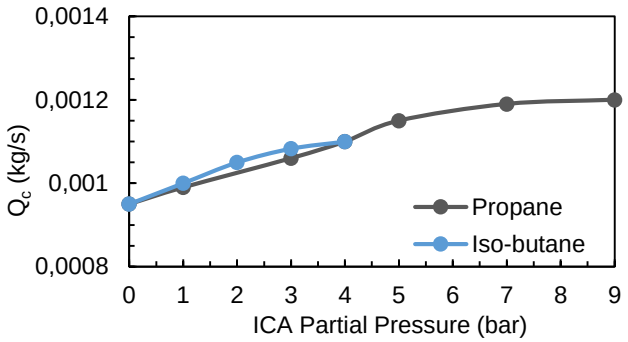

Figure 12. Effect of ICA on catalyst inlet flowrate. Values regarding simulation II.

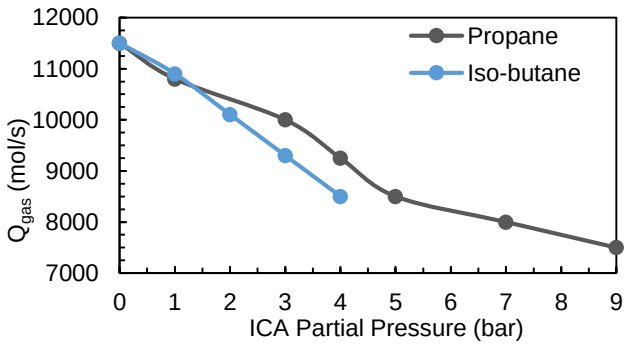

Figure 13. Effect of ICA on gas inlet flowrate. Values regarding simulation II.

Figure 14. shows that productivity of the catalyst decreases with the increase of the ICA partial pressure, but not because of the change in the ICA partial pressure. The decrease in catalyst productivity is related to the decrease of the inlet gas flowrate, which leads to less ethylene being available.

In Figure 15 the ethylene per pass conversion is shown. The same amount of PE is being produced, but a higher amount of catalyst is necessary to guarantee the production rate. The ethylene conversion is increasing, since a constant amount of PE is being produced, but the inlet flow of ethylene is decreasing.

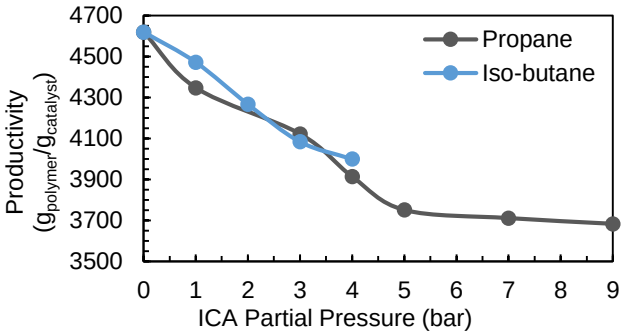

Figure 14. Effect of ICA on productivity. Values regarding simulation II.

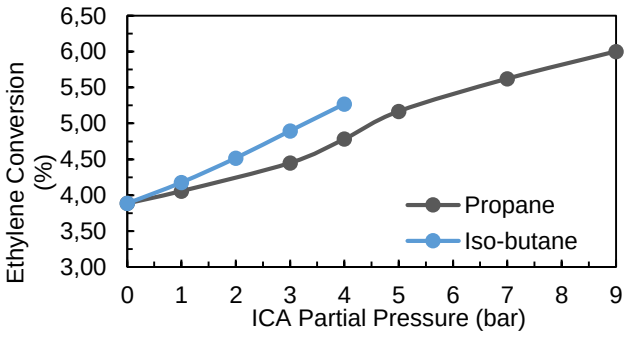

Figure 15. Effect of ICA on ethylene per pass conversion. Values regarding simulation III.

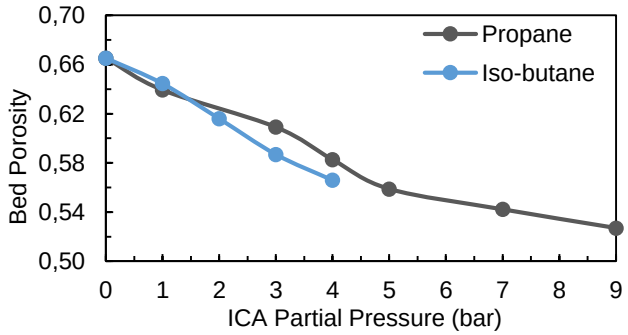

Figure 16. Effect of ICA on bed porosity. Values regarding simulation II.

There is a decrease in superficial velocity, due to the change in gas inlet flowrate. In this simulation the superficial velocity decreases from 0.95 to 0.6 m/s, which leads to a contraction of the bed, as seen in Figure 16. Even though there is a major decrease in gas inlet flowrate, the conditions still ensure full bed fluidization. Targeting the simulation with propane at 9 bar (lowest inlet gas flowrate), we can observe that the bed porosity remains well above the minimum fluidization porosity of 0,476.

Figure 17 shows the results for the polymer PSD. Analysing it, it becomes clear that the mean particle size increases with the presence of more ICA, contrasting Figure 10. Since the temperature is kept constant it is possible to observe the co-solubility effects, which lead to higher ethylene concentration in the polymer phase.

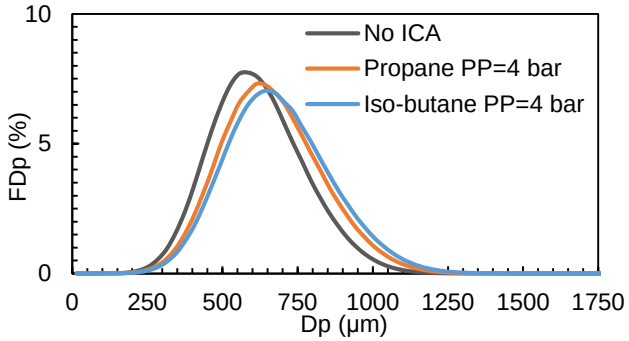

Figure 17. Effect of the ICA on polymer PDS for simulation II.

Simulation III

Simulation III allows to observe the effect of the ICA on the polymer PSD, since the simulations were ran using only the PSD model, keeping ethylene concentration and bulk temperature fixed.

When the temperature is kept constant at 80ºC, the ICA's used are n-hexane (partial pressure between 0-1 bar) and iso-butane (partial pressure between 0-4 bar).

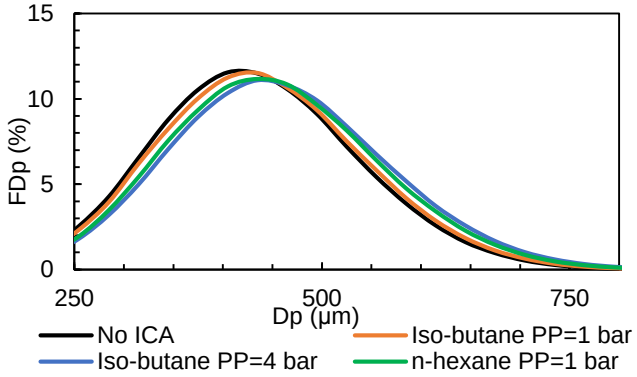

Figure 18. Effect of ICA on polymer PSD at 80ºC (zoomed). Values regarding simulation III

The difference caused by the ICA in the PSD is not very striking. It is clear that the increase of ICA leads to bigger particles. However, it is obvious that the heavier alkane (n-hexane) is responsible for a higher increase in the average particle size than the lighter alkane (iso-butane). This difference is so pronounced that to get similar PSD where the mean particle size increases 7% one must use 1 bar of n-hexane or 4 bar of iso-butane. This is a direct effect of co-solubility phenomena. The following Table shows the average particle sizes for each ICA.

Table 6. Average particle size for iso-butane and n-hexane at 80ºC.

	Partial pressure (bar)	Average particle size (µm)
No ICA	-	380
iso-butane	1	400
iso-butane	4	430
n-hexane	1	430

To further investigate about the temperature effect, Figure 19 shows a comparison of the polymer PDS using iso-butane at a partial pressure of 4 bar at 70ºC and 80ºC.

Figure 19 shows that the temperature is a parameter of much higher importance in the polymer PSD. Even though at 70ºC the concentration of ethylene in the polymer phase is higher than at 80ºC, the polymer still exhibits smaller particles. The average particle size increases 5% when the temperature is increased by 10 ºC.

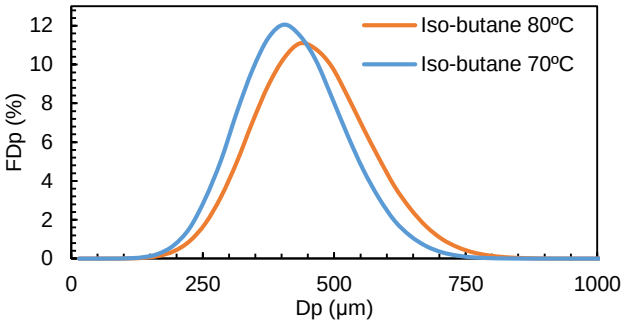

Figure 19. Effect of temperature in polymer PDS for iso-butane (partial pressure 4 bar).

Conclusions

A mathematical model was developed for the study of the impact of ICA on the production, reactor behaviour and polymer PDS.

The model has been validated and has shown a good agreement with chosen example.

The results show that all reactor parameters are sensitive to the presence of ICA. The presence of ICA increases the concentration of ethylene in amorphous polymer phase and decreases its density. When the inlet flow is maintained constant, the increase of ICA partial pressure decreases reactor temperature and increases productivity, production, ethylene conversion and pressure drop. When production and reactor temperature are kept constant, the gas inlet flowrate decreases, but an increase in catalyst inlet flow is observed. There is also bed contraction, due to the decrease in superficial velocity and an increase in the particle size. The temperature is shown to have a greater impact on polymer PSD than the effects of co-solubility.

In future development this model would benefit from:

- A PSD model that accounts for the catalyst sites deactivation;
- A detailed model for the bed fluidization;
- Modelling of the condensed mode operation;
- Incorporation of a reliable thermodynamic model that allows the user to consider more components in the reactor.

The evaluation of the cost/benefit of further developing this model by introducing more complexity is also an important issue to be taken into account.

References

[1] A. J. Peacock, *Handbook of Polyethylene: Structures: Properties and Applications*, 1st editio. CRC Press, 2000.

[2] J. B. P. Soares and T. F. L. McKenna, *Polyolefin Reaction Engineering*. Wiley-VCH, 2012.

[3] A. Wonders, G. E. Moore, R. R. Ford, F. D. Daily, K. A. Dooley, and J. J. Garcia, "Suppression of Fines in Fluid Bed Polyethylene Process," Patent US 5969061, 1999.

[4] R. E. Pequeno, R. O. Hagerty, and B. Savatsky, "Bulk Density Promoting Agents in a Gas-phase Polymerazation Process to Achieve a Bulk Particle Density," US 7754834 B2, 2010.

[5] T. Xie, K. B. McAuley, J. C. C. Hsu, and D. W. Bacon., "Gas phase ethylene polymerization: Production processes, polymer properties, and reactor modeling," *Ind. Eng. Chem. Res.*, vol. 33, no. 3, pp. 449–479, 1994.

[6] J. Davidson and D. Harrison, *Fluidized particles*. Cambridge University Press, 1963.

[7] D. Kunii and O. Levenspiel, *Fluidization Engineering*, 2nd editio. Reed Publishing Inc., 1991.

[8] Y. Wen-Ching, *Handbook of Fluidization and Fluid-Particle Systems*. CRC Press, 2003.

[9] K. Y. Choi and W. H. Ray, "The dynamic behavior of fluidized bed reactors for solid catalysed gas phase olefin polymerization," *Chem. Eng. Sci.*, vol. 40(12), pp. 2261–2279, 1985.

[10] W. E. Grosso and M. G. Chiovetta, "Modeling a fluidized-bed reactor for the catalytic polimerization of ethylene: particle size distribution effects," *Lat. Am. Appl. Res.*, vol. 35, pp. 67–76, 2005.

[11] H. Hatzantonis, H. Yiannoulakis, A. Yiagopoulos, and C. Kiparissides, "Recent developments in modeling gas-phase catalyzed olefin polymerization fluidized-bed reactors: the effect of bubble size variation on the reactor's performance," *Chem. Eng. Sci.*, no. 55, p. 3237, 2000.

[12] K. McAuley, J. P. Talbot, and T. Harris, "A Comparison of Two-Phase and Well Mixed Models for Fluidized Bed Polyethylene Rectors," *Chem. Eng. Sci.*, vol. 49(13), pp. 2261–2279, 1994.

[13] P. . J. T. Tait, *Comprehensive Polymer Science*. Oxford, 1989.

[14] L. Noristi, E. Marchetti, G. Baruzzi, and P. Sgarzi, "Investigation on the particle growth mechanism in propylene polymerization with MgCl2-supported ziegler–natta catalysts," *J. Polym. Sci., Part A Polym. Chemestry*, vol. 32, pp. 3047–3059, 1994.

[15] C. W. Hock, "How Ticl3 Catalysts Control the Texture of As-Polymerized Polypropylene," *J. Polym. Sci., Part A Polym. Chemestry*, vol. 3, no. 12, pp. 3055–3064, 1966.

[16] J. J. Boor, *Ziegler-Natta Catalysts and Polymerization*. New York: Academic Press, 1979.

[17] M. Kakugo, H. Sadatoshi, J. Sakai, and M. Yokoyama, "Growth of polypropylene particles in heterogeneous Ziegler-Natta polymerization," *Macromolecules*, vol. 22, no. 7, pp. 3172–3177, 1989.

[18] J. B. Soares and A. E. Hamielec, "Effect of reactor residence time distribution on the size distribution of polymer particles made with heterogeneous ziegler-natta and supported metallocene catalysts. a generic mathematical model," *Macromol. Theory Simulations*, vol. 4(6), pp. 1085–1104, 1995.

[19] P. Galli and J. C. Haylock, "Advances in Ziegler-Natta polymerization - unique polyolefin copolymers, alloys and blends made directly in the reactor," *Makromol. Chemie. Macromol. Symp.*, vol. 22, no. 1, pp. 19–54, 1992.

[20] K. B. McAuley, J. P. Talbot, and T. J. Harris, "A comparison of two-phase and well-mixed models for fluidized-bed polyethylene reactors," *Chem. Eng. Sci.*, vol. 49, no. 13, pp. 2035–2045, 1994.

[21] J. P. Talbot, "The Dynamic Modeling and Particle Effects on a Fluidized Bed Polyethylene Reactor," Queen's University, 1990.

[22] D. M. Cecílio, "Modelling of Gas and Slurry Phase Polyolefin Production : The importance of thermodynamics," 2015.

[23] Y. S. Wong and P. K. Seville, "Single-particle motion and heat transfer in fluidized beds," *AIChE J.*, vol. 52(12), pp. 4099–4109, 2006.

[24] S. Ergun, "Fluid Flow through Packed Columns," *Chem. Eng. Prog.*, vol. 48, 1952.

[25] J. M. Coulson and J. F. Richardson, *Chemical Engineering*. Bath Press, 2002.

[26] R. C. Reid, J. M. Prausnitz, and E. E. Poling, *The Properties of Gases & Liquids*, 4th ed. McGraw Hill.

[27] A. BRAGANCA, "Process for the gas phase polymerization and copolymerization of olefin monomers," 2005.

[28] A. Alizadeh, "Study of Sorption, Heat and Mass Transfer During Condensed Mode Operation of Gas Phase Ethylene Polymerization on Supported Catalyst," Queen's University, 2014.